FRONTIERS ARTICLE

Dynamics of excited state electron transfer at a liquid interface using time-resolved sum frequency generation

Yi Rao, Man Xu, Steffen Jockusch, Nicholas J. Turro, Kenneth B. Eisenthal *

Department of Chemistry, Columbia University, 3000 Broadway, New York, NY 10027, United States

ARTICLE INFO

Article history:
Available online 23 June 2012

ABSTRACT

Femtosecond time resolved vibrational sum frequency generation has been used for the first time to probe a chemical reaction involving interfacial molecules pumped into their excited electronic states. The ultrafast dynamics of electron transfer from ground state *N,N*-dimethylaniline (DMA) to photoexcited coumarin 314 at a water/DMA monolayer interface was obtained. The forward electron transfer time constant is 16 ± 2 ps, which is faster than electron transfer in bulk DMA. The faster rate is attributed to a lower reorganization free energy, which is a consequence of lower interfacial polarity. The back electron transfer time constant is 174 ± 21 ps.

1. Introduction

Electron transfer is a process of fundamental scientific and technological importance [1–7]. The physical and chemical characteristics of excited state electron transfer from a donor molecule to an excited state acceptor molecule, or the reverse, have been extensively studied since the discovery of excited state charge transfer complexes in bulk liquids [6–10]. The electron transfer reaction is a primary photophysical and photochemical process that provides new channels for energy degradation in excited state molecules producing an excited state charge transfer complex in low dielectric environments, which can emit fluorescence, intersystem cross to a triplet state, return of the donor and acceptor to their ground electronic states, or produce ion radicals in high dielectric environments [6–10]. A molecular level description of electron transfer at liquid interfaces would be of distinct interest in interfacial regions such as aqueous/biological cell membranes, the transport of chemical species, e.g. proteins, peptides, ions, DNA, and drugs, across a bilayer membrane, photo-electrochemistry, liquid/semiconductor junctions, and environmental aqueous/mineral and aerosol interfaces [2,3]. Ultrafast fluorescence upconversion and visible transient absorption spectroscopy have been employed to study photo-induced electron transfer in which an excited state electron acceptor captures an electron from a ground state electron donor in the bulk liquid [9–13]. In addition, transient IR and Raman spectroscopy have been used to gain insights into the correlation of electron transfer with molecular structure [14,15]. Measurements of the electron transfer dynamics in the heterogeneous environment of liquid interfaces have been carried out using spectroscopic and electrochemical methods

[13,16,17]. An issue of some importance in electrochemical experiments is that both liquids must contain supporting electrolytes [20]. As a consequence, diffusion and ion transport processes must be included in any interpretation of the data. Together with the development of the aforementioned experimental methods, the field of electron transfer processes has been significantly advanced by the development of theoretical models, which have proven to be important in advancing our understanding of electron transfer processes [1,18,19].

With the development of high intensity lasers the second order optical methods of second harmonic generation (SHG) [21–27], and sum frequency generation (SFG) [28–38], which have the invaluable feature of being interface selective, i.e. coherent SHG and SFG are dipole forbidden in centro-symmetric and isotropic environments, are now abundantly available. Because of this symmetry imposed restriction the much larger population of molecules in the bulk liquid do not generate coherent optical SHG or SFG signals, which would otherwise overwhelm an SHG or SFG signal from the small population of molecules located at the interface that separate the two bulk media.

In the work reported here the focus is the dynamics of excited state electron transfer at a liquid interface. The method used is time resolved SFG. In earlier work we used SHG to observe the dynamics of electron transfer at the same interface [17]. The increase in the electron affinity of coumarin 314 (C314) on photoexcitation to its lowest excited singlet state enables it to act as an electron acceptor with ground state DMA. DMA in particular was chosen because, in serving as the ground state donor molecule, it eliminates the need for translational motion to bring it into contact with the interfacial C314 molecules; DMA is already present at the interface. In early picosecond studies we used this approach to eliminate the need for translational motion for electron transfer to photoexcited anthracene from the electron

* Corresponding author.
  E-mail address: kbe1@columbia.edu (K.B. Eisenthal).

donating diethylaniline molecules by immersing anthracene in the bulk diethylaniline liquid [39,40].

2. Experimental section

A spectrally and time resolved visible-pump SFG-probe technique has been described previously [41–43]. Briefly, it entails combining a spectrally broad IR pulse, which is characteristic of femtosecond IR pulses, with a spectrally narrow visible pulse (12 cm^{-1}). The spectral resolution is determined by the spectral width of the narrow visible pulse. We achieve femtosecond time resolution by using femtosecond IR light and femtosecond pump pulses. The instrument response is determined by the cross correlation time of the IR and the pump light and was found to be 185 fs. An 800 nm regeneratively amplified Ti:sapphire system (Spitfire, Spectra Physics) seeded with a MaiTai 80 MHz, 80 fs oscillator, at a 1 kHz repetition frequency was employed in the present experiments. Two 800 nm femtosecond pulses were stretched to 10 ps to generate a 400 nm probe pulse by using a phase conjugation technique. The generated 400 nm pulse has a spectral width of 12 cm^{-1} and an output energy of 8 μJ per pulse. A tunable infrared light pulse between 3 and 8.5 μm with a bandwidth of 150 cm^{-1} was generated using part of an 800 nm femtosecond pulse with an OPA (Spectra-Physics). The remaining part of the 800 nm femtosecond pulse was used to generate a 423 nm femtosecond pump pulse with a second OPA.

The IR beam with a typical power of 1.5 μJ per pulse at 5.7 μm is focused onto the sample by a BaF$_2$ lens at an angle of 57° to the surface normal. The 400 nm picosecond light was focused at an angle of 76° to the surface normal. The 423 nm pump light was focused at an angle of 65°. The polarization of the pump beam was set to be S-polarized, which is perpendicular to the incident plane. The reason for the S-polarized pump is that it exhibits more efficient photoexcitation than other polarizations. A 300 mm spectrograph coupled to a CCD camera (Acton) was used to measure the SFG spectra, and a PMT (Hamamatsu) was used in the time-dependent measurements. The signal was boxcar gated, then sent to a phase-sensitive lock-in amplifier, and recorded by a computer (National Instruments A/D board), which controlled the delay between the pump and probe pulses via a stepper-motor driven translational stage (Klinger).

The electronic spectrum of C314 at the interface was measured by the SHG methods, in which the intensity of the second harmonic signal was recorded while tuning the fundamental wavelength of the probe laser beam. Non-resonant SHG signal from an x-cut quartz crystal interface was recorded as a reference for normalization to take into account laser intensity variation as the wavelength was tuned.

The chemical structures of C314 and DMA are shown in Scheme 1. The purity of C314 (99%, Aldrich) was checked by HPLC. A solution of 15 μM C314 and 8 mM DMA was prepared using ultrapure water (resistivity 18.2 MΩ cm, Millipore Corp.). DMA was used as received (99.5+%, Aldrich). The Teflon beakers were cleaned prior to use by immersion in freshly prepared piranha solution for 30 min and then rinsed with copious amounts of ultrapure water
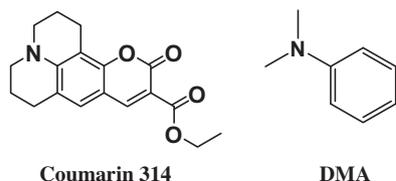
in order to remove any trace organics. The sample was contained in a shallow Teflon beaker mounted on a stage rotating at 2.5 rpm to minimize heating and degradation effects during laser irradiation.

3. Results and discussion

Here we briefly outline the theory of sum frequency generation as it applies to interfaces. We consider two incident laser pulses, one visible pulse and an IR pulse that can be tuned into resonance with a vibrational state of an interfacial molecule. The sum frequency intensity ($I(\omega_{SF})$) is proportional to the square of the sum of all sum frequency susceptibility terms separated into a resonant part, $\chi_R^{(2)}$, in which the IR is resonant with an interfacial molecule, and a part that is non resonant with the vibration, namely, $\chi_{NR}^{(2)}$. The SFG intensity is given by [44],

$$I_{SF}(t) \propto \left| \chi_{NR}^{(2)} + \chi_R^{(2)} \right|^2 I(\omega_{Vis})I(\omega_{IR}) = \left| \chi_{NR}^{(2)} + \sum_q \frac{A_q}{\omega_{IR} - \omega_q + i\Gamma} \right|^2 I(\omega_{Vis})I(\omega_{IR})$$

(1)

where A_q contains the product of the Raman and IR matrix elements of the qth normal mode, ω_q denotes the resonant frequency of the qth vibrational normal mode, ω_{IR} is the frequency of the IR light, and Γ_q is the spectral width of the vibrational state. In the case of dielectric interfaces, the contribution from the nonresonant parts is small compared to the resonant terms of interest.

Figure 1 shows that the SHG spectra of C314 molecules at the interface are blue shifted with respect to bulk DMA and bulk water, which indicates that the C314 molecules experience a lower polarity at the interface than in the bulk liquids. The SFG spectra for SSP polarization combinations were measured in each experiment, where the first letter (S) denotes the polarization of the sum frequency, the second one (S) denotes the polarization of the 400 nm light, and the last one (P) denotes the polarization of the IR light. These polarizations are connected with the laboratory coordinates by nonlinear Fresnel coefficients and appropriate projections [21,27,36,41,45,46]. Figure 2 shows that the main peak is at 1738 cm^{-1} in the SSP polarization spectrum with a weak peak at 1680 cm^{-1}. We assigned the main peak at 1738 cm^{-1} to the symmetric stretching mode of the —C=O in the ring of C314. The weak peak at 1680 cm^{-1} was shown to be the stretching mode of the carbonyl group of the ethyl ester [42]. The molecular orientation of the —C=O group in the ring of C314 was measured using

Scheme 1. The chemical structures of coumarin 314, C314, and N,N-dimethylaniline, DMA.
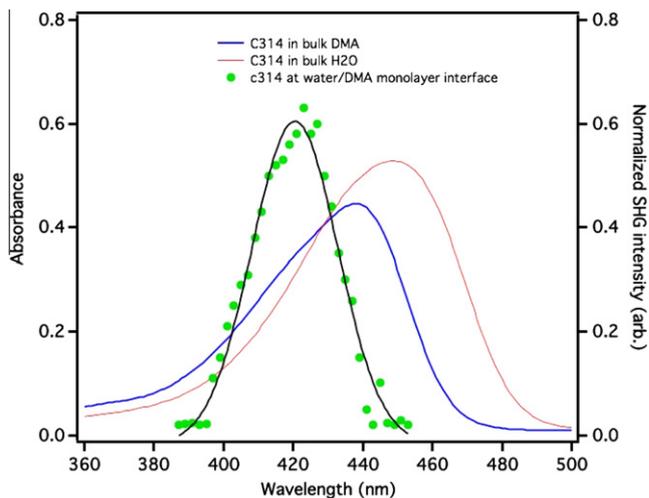
Figure 1. SHG spectrum of C314 molecules at the water/DMA monolayer interface (green solid circle) and UV spectra of C314 in bulk DMA (blue solid line) and in water (red solid line).
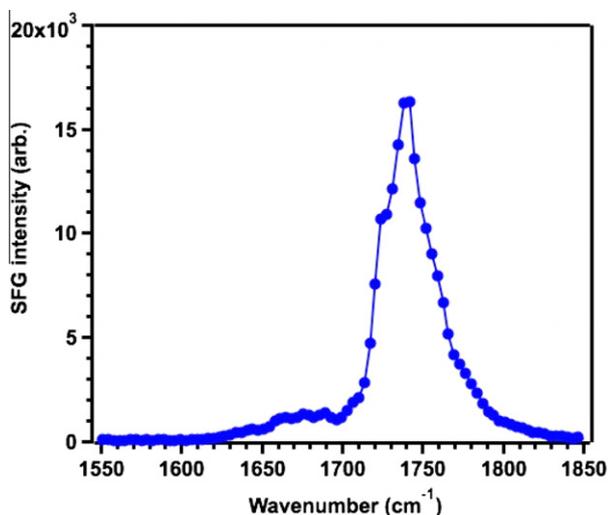
Figure 2. SSP SFG spectrum of C314 at the water/DMA monolayer interface (blue solid circle).

Figure 3. SSP SFG spectra of the ―C═O group of C314 at the water/DMA monolayer interface at different delay times with respect to the pump pulse.

the intensity ratio of SSP to PPP SFG intensities [42]. The angle of the carbonyl group of C314 in the presence of DMA, assuming a delta function distribution is ∼73° with respect to the surface normal, i.e. the carbonyl pointing towards to the bulk water.

A pump laser, which is resonant with the interfacial absorption peak of C314 molecules, was employed to excite a small fraction of the C314 interfacial molecules. While the pump can excite solute molecules beyond the surface, the technique only monitors the interfacial solute molecules due to the surface specificity of SFG. The time-dependent changes in the interface following the femtosecond photoexcitation of C314 were measured by monitoring the SFG signal generated by the probe pair, which overlap in time and space at the sample interface. The pair consists of a 400 nm picosecond pulse and a femtosecond IR pulse at 5.7 μm, which is resonant with the ring ―C═O stretch wavelength. There was no evidence that the frequency of the ring ―C═O stretch was different in the C314 excited state compared to its ground state value, i.e. no new feature was observed in scanning the incident IR frequency from 1550 to 1850 cm^{-1}. This is in agreement with previous results for the ―C═O group of coumarin 337 in the singlet state [15,47].

Upon photoexcitation of interfacial C314 molecules, the total SFG susceptibility consists of contributions from both ground and excited state molecules. The time dependent SFG intensity is given by [42,48],

$$I_{SF}(t) \propto \left| \chi_g^{(2)}(t) + \chi_e^{(2)}(t) \right|^2 I(\omega_{Vis})I(\omega_{IR}) \qquad (2)$$

The time-dependent ground state contribution, $\chi_g^{(2)}(t)$, and the time-dependent excited state contribution, $\chi_e^{(2)}(t)$, evolve as the solvent reorganizes about the newly excited C314 molecules. The electron transfer from the electron donor to the acceptor and the orientational dynamics of the donor and acceptor also change the SFG susceptibilities with time. Because the sum frequency generation is a coherent optical process, the two contributions interfere constructively or destructively, depending on their relative phases.

As shown in Figure 3, at a time delay of −1 ps, the probe pulses precede the pump light, and the SFG spectrum corresponds to that without pumping. The SFG intensity at the peak 1738 cm^{-1} decreased when the pump beam and the probe beams overlapped at t = 0 due to photobleaching of the ground state C314 molecules and the interference due to the excited state C314 having a phase that differs from that of the ground state C314 by π/2 to π. Figure 4 shows time profiles of SFG fields for C314 without and with DMA
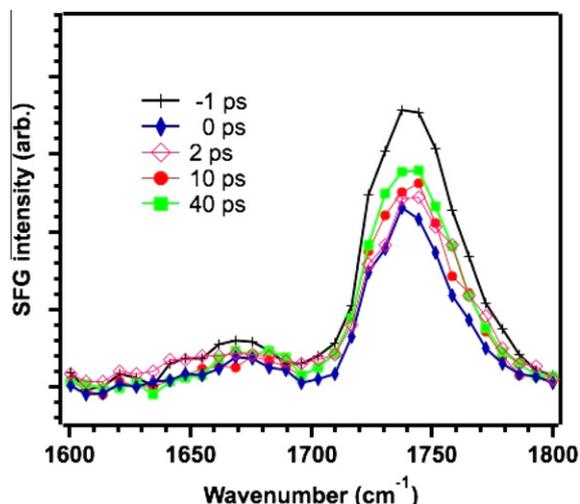
at interfaces following photoexcitation of C314. The SFG field is seen to decrease both without and with DMA within the instrumental response time of 185 fs. Following photoexcitation of C314 with a polarized pump pulse the dynamic processes that ensue in the presence of DMA include: (i) reorganization of the interfacial solvent molecules about the newly excited C314 molecules, i.e. solvation dynamics, (ii) rotation of excited state C314 and ground state C314 molecules, during which time some will achieve a reaction geometry, (iii) electron transfer from DMA to an excited state C314, which can take place because of the increased electron affinity of C314 on photoexcitation, (iv) rotational motions of the ground state C314 molecules, whose equilibrium orientational distribution had been perturbed by the polarized pump photoexcitation, back to their equilibrium distribution; the photoselection of the C314 molecules by the pump pulse does not perturb the equilibrium orientation of the DMA molecules at the interface because the DMA does not absorb the pump light, (v) rotation of the photoexcited molecules to their equilibrium distribution, and (vi) back electron transfer from the coumarin radical anion, C314⁻·, to the dimethylaniline radical cation, DMA⁺·, generating ground state
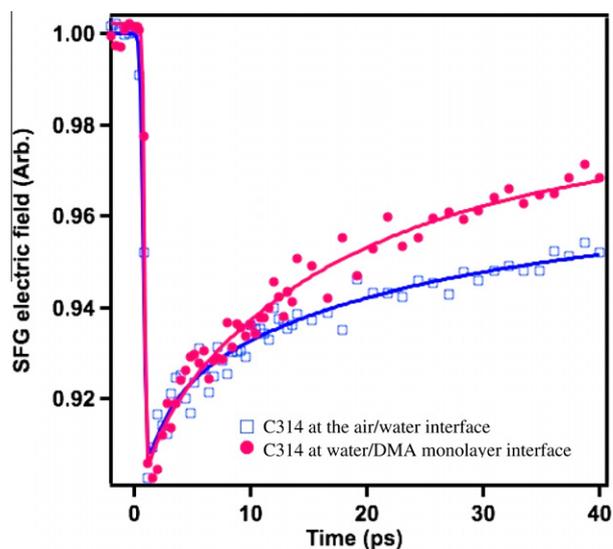

Figure 4. Time profiles of the C314 SFG electric fields at the water/DMA monolayer (red solid circle) and air/water (blue square) interfaces. The solid lines are fits of the data.

C314 and DMA. As seen in Figure 4 the rate of recovery of the SFG field is faster in the presence of DMA. However, at short times after photoexcitation, i.e. a few picoseconds, the dynamics of recovery is the same with and without DMA. This indicates that the solvation dynamics controls the recovery in the first few picoseconds [43] and that the electron transfer from ground state DMA to excited state C314 is slower and does not contribute to the dynamics in the first few picoseconds. At later times, the dynamics is that of forward electron transfer from ground state DMA to excited state C314, generating the C314 radical anion and the DMA radical cation. Following this electron transfer quenching of the excited state C314 molecules, the back electron transfer from the C314 radical anion to the DMA radical cation takes place. A complicating feature of the dynamics at long times is that the time scale of the back electron transfer overlaps with the rotational dynamics of C314. The newly formed C314 molecules and the C314 molecules that were not excited by the polarized pump pulse, undergo rotations that ultimately lead to their equilibrium orientational distribution. It is also noted that with the probe pair that we are using, the SFG signal is sensitive to the population and orientation of the C314 molecules. In order to separate the back electron transfer from the rotational dynamics of C314 we measured the orientational relaxation time of C314 at an interface of water with a liquid that does not undergo electron transfer to excited state C314 molecules, and whose viscosity is close to that of DMA. We selected benzonitrile, which is a liquid at room temperature and has a viscosity of 1.24 cp at 25 °C that is close to that of DMA, 1.29 cp at 25 °C. The rotation time of C314 at the water/benzonitrile monolayer interface was found to be 245 ± 20 ps.

The longer time behavior, in Figure 5, shows the SFG field to be very close to its value before photoexcitation, which indicates that the C314 interfacial molecules have almost completely returned to their ground states and to their equilibrium orientational distribution. The best fit of the data subsequent to solvation yielded three components. The faster one is 16 ± 2 ps, (amplitude 0.7), which is attributed to the forward electron transfer dynamics. The SFG signal is seen to increase with time as the excited state C314 molecules react with DMA because the phase of the C314 excited state is opposite to ground state C314, and therefore reduces the total SFG signal (see Eq. (2)). The second one is 174 ± 21 ps (amplitude 0.2), which is attributed to the back electron transfer dynamics. The third component is the rotational dynamics obtained using benzonitrile with an amplitude of 0.1. These results are in excellent agreement with our SHG measurements of the same system [17].
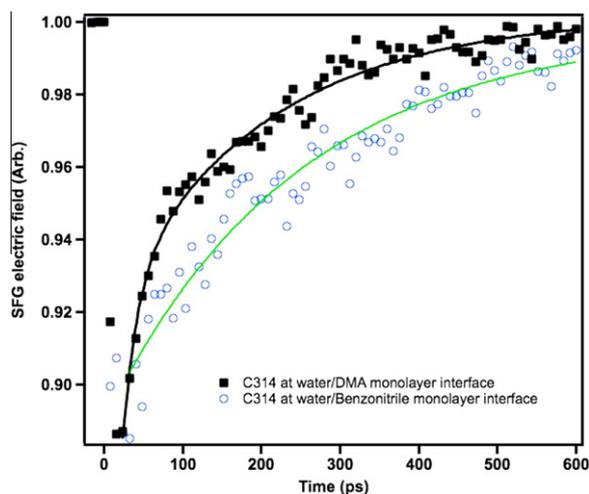

Figure 5. Time profiles of the C314 SFG electric fields at the water/DMA monolayer (black solid square) and water/benzonitrile monolayer (blue circle) interfaces. The solid lines are fits of the data.

In the SHG experiments the forward electron transfer dynamics was measured in two ways. In one the probe light was resonant with the C314 $S_0 \rightarrow S_1$ transition. As a consequence, it is the C314 molecules that are the dominant contributor to the SHG signal. The forward electron transfer was found to be 14 ± 2 ps [17], which is in excellent agreement with the SFG result of 16 ± 2 ps. A direct confirmation that the dynamics was due to forward electron transfer was obtained by tuning the probe light to a frequency that was resonant with an electronic transition in the DMA radical cation. In this SHG experiment, the observed rise time of DMA$^{+\cdot}$ is determined by the dynamics of electron transfer from ground state DMA to excited state C314, producing the C314$^{-\cdot}$ radical anion and the DMA$^{+\cdot}$ radical cation. The time constant of DMA$^{+\cdot}$ formation is 16 ± 3 ps. Thus we see that the dynamics of forward electron transfer obtained from SHG measurements of the decay of C314$^{-\cdot}$ and from SHG measurements of the formation of DMA$^{+\cdot}$ are in excellent agreement. In order to compare interfacial forward electron transfer dynamics with that in bulk DMA requires knowledge of the bulk dynamics, which we do not have. However, we do have results on the forward electron transfer rate constant at the water/DMA monolayer interface for coumarin 153 (C153) which we obtained from SHG measurements [17,49], and knowledge of the C153 rate constant in bulk DMA [50]. Our results show that the forward electron transfer at the interface is faster than that of C153 in bulk DMA. The C153 molecule is structurally very similar to C314, and has a reduction potential that is only 0.01 ev larger than that of C314 [17,49]. Furthermore our SHG measurements of the forward electron transfer time constants for both C314 and C153 were equal within experimental error [49]. Based on these aforementioned observations we view the C314 dynamics in bulk DMA to be the same as C153, which permits the inference that C314 forward electron transfer at the interface is faster than in bulk DMA.

The key factors that determine the dynamics of electron transfer are the reorganization energy and the electron coupling between the donor and acceptor molecules. The lower polarity at the interface manifested by the blue shift of the C314 spectrum at the interface relative to bulk DMA, Figure 1, suggests that the reorganization free energy at the interface is less than in bulk DMA. This would therefore favor a more rapid electron transfer at the interface. Acting in the opposite direction is the electronic coupling between the donor and acceptor molecules, an interaction that is dependent on their separation and relative orientation. Because the density of DMA molecules surrounding a C314 molecule is higher in the bulk liquid than at the interface, it follows that there are more donor molecules close to C314, which would therefore contribute to a faster electron transfer in the bulk liquid. One might anticipate that among the large number of DMA molecules surrounding a C314 molecule in bulk DMA there could be more that have orientations such that they can serve as electron donors, than is the case for the lower density of DMA molecules at the interface. This last observation concerning relative orientation must be qualified because both the C314 and DMA molecules at the interface are oriented with respect to the interface normal of C314, and may already have a favorable orientation for electron transfer before excitation. As reported earlier in this Letter we have found that the orientation of the —C=O group in C314 in the presence of DMA is ~73°. To address this issue we plan to measure the interfacial orientation of ground state DMA at the interface in the presence of C314.

4. Conclusions

We have studied electron transfer at interfaces utilizing femtosecond time-resolved SFG. Surface-active C314 molecules pumped to excited electronic states served as electron acceptors with

respect to donor *N,N*-dimethylaniline molecules, at a water/DMA monolayer interface. Because of the immiscibility of DMA and water, the DMA molecules are at the interface and translational diffusion of interfacial C314 and DMA is not required. The electron transfer process was monitored by detection of the C314 carbonyl SFG signal. The time constant of the forward electron transfer process was found to be 16 ± 2 ps, which is approximately twice as fast as the forward electron transfer of a closely related on photo-excitation of a closely related coumarin in bulk DMA. The faster rate at the interface is attributed to the interface having a lower polarity than bulk DMA; this is supported by the measured blue shift of C314 at the interface in the presence of DMA with respect to the spectrum of C314 in bulk DMA. As a consequence of the lower polarity it is surmised that the free energy of reorganization is smaller at the interface, which would favor a faster electron transfer at the interface. It is concluded, on comparing the electron transfer rates at the interface and bulk DMA that the free energy of reorganization dominates the electronic coupling factor that could favor a faster rate in bulk DMA because there are more DMA molecules surrounding C314 in the bulk liquid. The back electron transfer process in which an electron is returned from the C314 radical anion to the DMA radical cation was found to have a time constant of 174 ± 21 ps. There was no evidence that the frequency of the ring —C=O stretch vibration was different in excited state C314 from its value in ground state C314. To our knowledge, this is the first time-resolved SFG experiment to examine electron transfer at a liquid interface.

Acknowledgments

References

[1] R.A. Marcus, J. Chem. Phys. 24 (1956) 966.
[2] J.R. Bolton, N. Mataga, G. McLendon (Eds.), Electron Transfer in Inorganic, Organic, and Biological Systems, American Chemical Society, Ottawa, Washington, DC, 1991.
[3] J. Jortner, M. Bixon, Electron Transfer- from Isolated Molecules to Biomolecules, J. Wiley, New York, 1999.
[4] A.W. Adamson, A.P. Gast, Physical Chemistry of Surfaces, John-Wiley & Sons Inc., 1997.
[5] M. Gratzel, Heterogeneous Photochemical Electron Transfer, CRC Press, Boca Raton, Fla, 1989.
[6] H. Leonhardt, A. Weller, Ber. Bunsenges. Phys. Chem. 67 (1963) 791.
[7] J.A. Syage, P.M. Felker, A.H. Zewail, J. Chem. Phys. 81 (1984) 2233.
[8] T.J. Chuang, K.B. Eisenthal, J. Chem. Phys. 59 (1973) 2140.
[9] K.B. Eisenthal, Acc. Chem. Res. 8 (1975) 118.
[10] T.J. Chuang, K.B. Eisenthal, J. Chem. Phys. 62 (1975) 2213.
[11] K. Weidemaier, H.L. Tavernier, S.F. Swallen, M.D. Fayer, J. Phys. Chem. A 101 (1997) 1887.
[12] E.W. Castner, D. Kennedy, R.J. Cave, J. Phys. Chem. A 104 (2000) 2869.
[13] M.A. Fox, Photoinduced electron transfer, Elsevier, New York: Distributors for the United States and Canada, Amsterdam, 1988.
[14] R.R. Frontiera, J. Dasgupta, R.A. Mathies, J. Am. Chem. Soc. 131 (2009) 15630.
[15] C.F. Wang, B. Akhremitchev, G.C. Walker, J. Phys. Chem. A 101 (1997) 2735.
[16] A.L. Barker, P.R. Unwin, S. Amemiya, J.F. Zhou, A.J. Bard, J. Phys. Chem. B 103 (1999) 7260.
[17] E.A. McArthur, K.B. Eisenthal, J. Am. Chem. Soc. 128 (2006) 1068.
[18] I. Benjamin, E. Pollak, J. Chem. Phys. 105 (1996) 9093.
[19] J. Vieceli, I. Benjamin, Chem. Phys. Lett. 385 (2004) 79.
[20] AJ. Bard, L.R. Faulkner, Electrochemical Methods: Fundamentals and Applications, Wiley, 2000.
[21] Y.R. Shen, Nature 337 (1989) 519.
[22] K.B. Eisenthal, Annu. Rev. Phys. Chem. 43 (1992) 627.
[23] J.C. Conboy, J.L. Daschbach, G.L. Richmond, Appl. Phys. A-Mater. 59 (1994) 623.
[24] Y. Rao, Y.S. Tao, H.F. Wang, J. Chem. Phys. 119 (2003) 5226.
[25] W.H. Steel, R.A. Walker, Nature 424 (2003) 296.
[26] H.F. Wang, E. Borguet, K.B. Eisenthal, J. Phys. Chem. B 102 (1998) 4927.
[27] T.F. Heinz, H.W.K. Tom, Y.R. Shen, Phys. Rev. A 28 (1983) 1883.
[28] M.J. Shultz, C. Schnitzer, D. Simonelli, S. Baldelli, Int. Rev. Phys. Chem. 19 (2000) 123.
[29] C.S. Santos, S. Baldelli, J. Phys. Chem. C 112 (2008) 11459.
[30] G. Ma, J. Liu, L. Fu, E.C.Y. Yan, Appl. Spectrosc. 63 (2009) 528.
[31] J. Kim, K.C. Chou, G.A. Somorjai, J. Phys. Chem. B 107 (2003) 1592.
[32] W. Gan, D. Wu, Z. Zhang, R.R. Feng, H.F. Wang, J. Chem. Phys. 124 (2006) 114705.
[33] F.M. Geiger, Annu. Rev. Phys. Chem. 60 (2009) 61.
[34] M.C. Gurau, E.T. Castellana, F. Albertorio, S. Kataoka, S.M. Lim, R.D. Yang, P.S. Cremer, J. Am. Chem. Soc. 125 (2003) 11166.
[35] O. Esenturk, R.A. Walker, J. Phys. Chem. B 108 (2004) 10631.
[36] H.F. Wang, W. Gan, R. Lu, Y. Rao, B.H. Wu, Int. Rev. Phys. Chem. 24 (2005) 191.
[37] J.T. Fourkas, R.A. Walker, S.Z. Can, E. Gershgoren, J. Phys. Chem. C 111 (2007) 8902.
[38] A.N. Bordenyuk, A.V. Benderskii, J. Chem. Phys. 122 (2005) 134713.
[39] K. Gnadig, K.B. Eisenthal, Chem. Phys. Lett. 46 (1977) 339.
[40] T.J. Chuang, R.J. Cox, K.B. Eisenthal, J. Am. Chem. Soc. 96 (1974) 6828.
[41] Y. Rao, M. Comstock, K.B. Eisenthal, J. Phys. Chem. B 110 (2006) 1727.
[42] Y. Rao, D.H. Song, N.J. Turro, K.B. Eisenthal, J. Phys. Chem. B 112 (2008) 13572.
[43] Y. Rao, N.J. Turro, K.B. Eisenthal, J. Phys. Chem. C 114 (2010) 17703.
[44] X. Zhuang, P.B. Miranda, D. Kim, Y.R. Shen, Phys. Rev. B 59 (1999) 12632.
[45] Y. Rao, M. Subir, E.A. McArthur, N.J. Turro, K.B. Eisenthal, Chem. Phys. Lett. 477 (2009) 241.
[46] Y. Rao, N.J. Turro, K.B. Eisenthal, J. Phys. Chem. C 113 (2009) 14384.
[47] B. Akhremitchev, Laser Chem. 19 (1999) 403.
[48] Y. Rao, S.Y. Hong, N.J. Turro, K.B. Eisenthal, J. Phys. Chem. C 115 (2011) 11678.
[49] E.A. McArthur, Ph.D. Thesis, 2008.
[50] H. Shirota, H. Pal, K. Tominaga, K. Yoshihara, J. Phys. Chem. A 102 (1998) 3089.

Yi Rao received a Ph.D. in physical chemistry from Institute of Chemistry, Chinese Academy of Sciences in 2003. In 2004, he joined Professor K. B. Eisenthal's group as a postdoctoral research fellow at Columbia University. Since 2007, he has been an associate research scientist at Columbia University, collaborating with Professors Nicholas J. Turro and Kenneth B. Eisenthal.
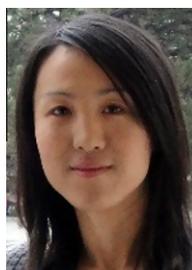
Man Xu received her B.S. and M.S. in chemistry and environmental science from Nanjing University in China and a Ph.D. in environmental science from The Ohio State University. After graduation, Man continued her research in surface chemistry at Columbia University and later at Wright State University. She is currently a postdoctoral research associate at the Pacific Northwest National Laboratory.

Steffen Jockusch received his Ph.D. degree from the Martin Luther University Halle-Wittenberg in Merseburg (Germany). In 1994, he joined Prof. Turro's research group at Columbia University as a postdoctoral fellow, and since 1997, he has been an associate research scientist.

Nicholas J. Turro is currently the Wm. P. Schweitzer Professor of Chemistry at Columbia University where he has been since 1964. He has written over 900 scientific publications and 3 textbooks on molecular photochemistry. He is a member of the National Academy of Sciences and the American Academy of Arts and Sciences.

Kenneth B. Eisenthal received a B.S. in chemistry from Brooklyn College and an M.A. in physics and a Ph.D. in chemical physics from Harvard University. He did postdoctoral research at UCLA and was at IBM Almaden Research Division Laboratory before coming to Columbia University in 1975. He is a member of the National Academy of Sciences.